Journal of Nuclear Materials 380 (2008) 59–69

Contents lists available at ScienceDirect

Journal of Nuclear Materials

journal homepage: www.elsevier.com/locate/jnucmat

Chemical durability of hollandite ceramic for conditioning cesium

Frédéric Angeli [a,*], Peter McGlinn [b], Pierre Frugier [a]

[a] CEA Marcoule, DEN/DTCD/SECM/LCLT, F-30207 Bagnols-sur-Cèze, France
[b] ANSTO, New Illawarra Road, Menai, PMB1, NSW 2234, Australia

ARTICLE INFO

Article history:
Received 7 March 2008
Accepted 15 July 2008

ABSTRACT

The aqueous corrosion behavior of Cs-doped hollandite ceramic ($BaCs_{0.28}Fe_{0.82}Al_{1.46}Ti_{5.72}O_{16}$) was studied using several different static experimental protocols, with leachants of varying pH, and at different surface area to volume ratios, for periods ranging from six months to three years. All leach tests were carried out at 90 °C. X-ray diffraction (XRD) and scanning electron microscopy (SEM), coupled with energy dispersive X-ray spectroscopy (EDS), were used to characterize the surfaces of the hollandite before and after leaching. The most pronounced elemental releases, and corresponding changes to surface composition and microstructure, was evident at low pH, in particular pH 1. Cs and Ba releases were highest at low pH, with surface alteration exhibited by the formation of secondary rutile (prevalent at pH 1) and Al- and Ba-depleted hollandite (prevalent at pH 2). After rapid initial Cs release, the alteration rate was extremely low over the pH range from 2 to 10, as well as in pure water experiments with a sample-surface-area-to-solution-volume ratio ranging from 0.1 cm^{-1} to 1200 cm^{-1}. The rates were about 10^{-5} g m^{-2} d^{-1}, corresponding to alteration thicknesses of a few nanometers per year. Higher rates (5×10^{-3} g m^{-2} d^{-1}) were observed only under very acidic conditions (pH 1). Congruency in Cs and Ba releases occurred only at pH 1, with incongruency between the two elements increasing with increasing pH. There were no apparent solubility constraints on Cs releases regardless of the SA/*V* ratio, whereas geochemical modeling suggested that Ba releases could have been affected by the formation of $BaCO_3$, particularly at high SA/*V* ratios. Extended leaching (with the leachant renewed once after 261 days of leaching) confirmed the high durability of hollandite with altered thicknesses of less than one nanometer per year over the last two years. Whilst Cs depletion of the hollandite surface was evidenced when leachates were replenished with the fresh deionised water, the presence of a soluble Ba-bearing secondary phase was inferred.

1. Introduction

Hollandite is one of the major phases of Synroc, a multiphase ceramic matrix also containing zirconolite and perovskite phases [1] that is being considered as a matrix for immobilizing Cs resulting from enhanced separation of fission product solutions from spent fuel reprocessing [2]. The advantage of this material is that it also incorporates Ba, a decay element of Cs. It also exhibits good thermal conductivity [3], an advantage due to the radiogenic heat produced by the decay of ^{137}Cs and ^{134}Cs, as well as good electronic irradiation resistance [4].

The hollandite formula proposed for Cs immobilization is $Ba_x^{2+}Cs_y^{+}M_{2x+y}^{3+}Ti_{8-2x-y}^{4+}O_{16}$ ($x \leqslant 2$) in which M is a trivalent cation, for example Ti^{3+}, Al^{3+} or Fe^{3+}, ensuring the charge compensation necessary for loading Ba and Cs. With Ti^{4+}, it forms octahedra that create a tunnel structure in which mono- or divalent cations (Cs and Ba, respectively) are inserted. The composition used in this study was a ferriferous hollandite containing Al: $Ba_1Cs_{0.28}Fe_{0.82}Al_{1.46}Ti_{5.72}O_{16}$ (which corresponds to the following oxide mass composition: 19.4% BaO, 5% Cs_2O, 8.3% Fe_2O_3, 9.4% Al_2O_3, 57.9% TiO_2). Adding iron allows pressureless consolidation (in air) through better control of the redox conditions during the synthesis process, without subsequently degrading the chemical durability of the matrix [5].

This type of composition contains no soluble secondary phases [6]. This point is of particular importance for hollandite disposal in a geological formation as the conditioning matrix must be resistant to aqueous dissolution with radioelement retention properties minimizing their release into the environment. Hollandite formulations are known for their good aqueous corrosion resistance [5–9]. After leaching Fe-free hollandite in deionized water at 75 °C and 150 °C, Pham et al. [8] reported very rapid initial release of Ba and Cs followed by dissolution of the upper atomic layers. The leach rate then dropped by at least an order of magnitude over the ensuing week. This was attributed to the formation of a thin passivating layer rich in Al and Ti. The authors noted a drop in the pH due to hydrolysis of Al, which reportedly precipitated on the surface as AlOH and/or $Al(OH)_3$. Carter et al. [6] measured very low Cs and Ba leach rates—below 0.001 g m^{-2} d^{-1} after 56 days at 90 °C in pure

* Corresponding author.
E-mail address: frederic.angeli@cea.fr (F. Angeli).

0022-3115/$ - see front matter © 2008 Elsevier B.V. All rights reserved.
doi:10.1016/j.jnucmat.2008.07.003

water—and reported a very slight effect of the solution pH (within the range between 2.5 and 12.9) on the Ba dissolution rate.

Under extremely acidic pH conditions obtained with a nitric acid solution (pH 0 and 1) and under hydrothermal conditions (200 °C), 100% of the Cs (and 90% of the Ba) can be leached in a few days (with a mean particle size of 10 microns) from hollandite $Cs_{0.8}Ba_{0.4}Ti_8O_{16}$ [9]. The main reaction products observed by X-ray diffraction (XRD) were first brookite then, after 95 h of leaching, mainly rutile. The authors noted that the percentage of Cs released at pH 2 was lower by a factor of about four if the pH was adjusted with HCl rather than HNO_3. The presence of an oxidizing agent (NO_3^-) suggests that oxidation of Ti^{3+} is an important process in the leaching mechanism. The slight difference in the specific surface area of the powder determined by N_2 adsorption before and after leaching shows that the formation of rutile is attributable to reorganization of the hollandite lattice after the release of Cs rather than to a dissolution–precipitation mechanism. The authors observed no secondary phases on the surface of the crystallites, but rather a continuous alteration front. The results suggest that the separation from the pristine hollandite occurs abruptly, without a Cs gradient. In addition, the Cs release was proportional to the number of Ti^{3+} cations oxidized to Ti^{4+}. The authors refer to Bursill's work [10] in proposing a mechanism by which hollandite is converted to rutile after the release of Cs, without Ti entering solution. They postulate that the conversion is initiated by oxidation of Ti^{3+}, entailing the extraction of Cs necessary to maintain neutrality. The Cs release would destabilize the tunnel structure with an alteration front being created by the formation of rutile and/or brookite. As the front progresses, Cs extraction becomes increasingly difficult.

There is a lack of data in the literature, however, concerning more moderate pH and temperature ranges, under long term leaching in which the alteration rates are difficult to measure. The purpose of this work was to investigate the behavior of a single-phase, Cs-bearing ferriferous hollandite (French reference) under leaching conditions more representative. Experiments were carried out over a wide range of pH and SA/V ratios, and for extended periods of time greater than 3 years (with complete leachate replacement after 261 days). Under steady-state conditions, the release of elements in solution as a function of SA/V ratio can infer alteration mechanisms e.g. if diffusion within the solid is one of the factors controlling the alteration rate the release of elements into solution would not be dependent on the solution chemistry (compared to a solubility controlled mechanism) and should therefore become proportional to surface area (i.e. SA/V ratio). Conversely, in a case of solubility control, the concentration of the elements in solution would be independent of the SA/V ratio in the medium to long term.

2. Experimental methods

2.1. Sample preparation

The hollandite was prepared by a wet process to ensure suitable mixing of the precursors (100–200 g) by blending an aqueous solution of Cs and Fe nitrates and Ba acetate with a solution containing Ti and Al alkoxides diluted in ethanol (when the two solutions were mixed, the hollandite precursor precipitated), then the solvent is evaporated in a rotary evaporator, followed by recovery and drying of the powder for 24 h at 120 °C before calcining for 5 h at about 1000 °C to obtain the hollandite phase. The calcine was then ground (wet milling for 1 h at 300 rpm) and pelletized at room temperature using uniaxial pressing at a pressure of 100 MPa. The pellets were sintered in air for 15 h at 1250 °C. The pellet density was 95% of theoretical density. The powder samples for leach test were prepared by grinding and sieving. Each particle size fraction was washed by sedimentation in acetone. The size fractions used in this study are indicated in Table 1 with their specific surface area as determined by krypton adsorption using the BET (Brunauer Emmett Teller) method [11].

2.2. Chemical durability tests

Two series of extended (3-year) closed-system experiments were carried out with hollandite powders (some monoliths have been added to the powders for surface characterization): one to assess the effect of the pH on alteration, the other concerning the effect of the sample-surface-area-to-solution-volume (SA/V) ratio. In the first series the leaching solution pH ranged from 1 to 10 while the SA/V ratio remained constant at 1 cm^{-1} (V = 1 L). In the second series, carried out in deionised water, the SA/V ratios ranged from 0.1 cm^{-1} to 1200 cm^{-1} (V = 1 L at 0.1 and 1 cm^{-1}, V = 0.5 L at 10 and 80 cm^{-1} and V = 0.1 L at 1200 cm^{-1}). Specific surface areas are derived from the BET measurements.

The static tests were carried out in PTFE reactors at 90 °C. The tests began when the powder specimen was placed in the reactor, which had previously been filled with leaching solution heated to 90 °C. The solutions for the controlled pH experiments were prepared from ultrapure water and NormaPur® HNO_3 (10^{-1}–10^{-4} M) and NaOH (4×10^{-3}–4×10^{-5} M) solutions. The pH was then adjusted for each sample. The leaching solutions were filtered at 0.45 μm, acidified by HNO_3 and analyzed by ICP-MS.

The normalized mass loss $NL_{(i)}$ calculated for element i is expressed as follows:

$$NL_{(i)} = \frac{C_{(i)} \cdot V}{SA \cdot x_{(i)}}.$$

When corrected for the solid/solution contact surface area SA, material density ρ and weight percentage of element i in the material $x_{(i)}$, the concentrations $C_{(i)}$ measured in a solution of volume V corresponds to an equivalent altered sample thickness:

$$e_i = \frac{c_i}{SA/V \cdot x_i \cdot \rho}.$$

The thickness e_i is significant only if element i is not retained in the alteration film. Considering the thin layers of hollandite that can be altered, no solid analysis is available that could attest that there is no Cs retention in the altered film. Nevertheless, the experiments described here (effect of the SA/V ratio) demonstrate the absence of any Cs recondensation mechanism—even at concentrations exceeding a 100 mg L^{-1}. Consequently, Cs can be considered as a hollandite alteration tracer.

2.3. Surface characterization

XRD was used to determine the purity of the hollandite before experimentation. The XRD used was a Panalytical X'Pert MPD-Pro ($\lambda_{Cu\ k\alpha 1}$ = 0.15405 nm). After leaching under the various pH conditions, XRD was used to examine the surface of the specimens to determine the nature of any alteration that may have occurred. In this case the XRD used was a Siemens D500 diffractometer using Co Kα-radiation (0.17903 nm) and fitted with a graphite monochromator and proportional counter.

Scanning electron microscopy (SEM), incorporating an energy dispersive X-ray spectrometer (EDS), was used to characterize

Table 1
Specific surface area of particle size fractions

Particle size range (μm)	Specific surface area ($m^2\ g^{-1}$)	Uncertainty ($m^2\ g^{-1}$)
20–40	0.757	0.053
40–63	0.273	0.019
63–125	0.089	0.006

the un-leached specimens and those leached at the different pHs. SEM was carried out with a JEOL JSM-6300 instrument operated at 15 kV, and fitted with a NORAN Voyager IV X-ray microanalysis system.

3. Results and discussion

3.1. Surface characterization of pristine hollandite

The XRD spectra are typical of single-phase hollandite with no other detectable phases present. There is some slight peak shift in the higher end of the spectra.

SEM carried out on the un-leached hollandite (see Table 2) indicates that there is approximately 15% porosity (see Fig. 1(a)). This increase of porosity (pellet density was 95%) is probably due to removal of grains during preparation of the specimens for SEM examination. The results show that is essentially single-phase hollandite with a minor phase present, 1–2% by volume, characterized by a larger Cs peak, with a much less significant Si peak. Due to the fineness of these particles (see Fig. 1(b)) it was not possible to confirm their composition exactly. Previous unpublished investigations by co-workers found a similar Cs–Si-rich phase present in hollandite ceramics, formed due to inadvertent contamination from the sample or agate materials used in preparing for fabrication.

3.2. Durability tests

3.2.1. Static leaching at different pH

Fig. 2 shows the normalized mass losses for Cs and Ba at the various pHs. The final pH value after 261 days of leaching was similar to the initial value in all cases (less than one pH unit difference). Following the rapid immediate release of Cs and Ba, the alteration rates decreased to about 10^{-5} g m^{-2} d^{-1} in most cases after a few tens of days for all pH conditions. The rapid instantaneous releases is partly attributable to the relatively soluble Cs–Si-rich trace phase present in the batch of hollandite used in these studies (see the surface characterization description). The normalized Cs mass losses were similar for all pH conditions over the entire leaching time, except for the longer term at pH 1 where the leaching rate between 56 and 261 days, calculated from the Cs release, was 5×10^{-3} g m^{-2} d^{-1}, about an order of magnitude higher than those for the other pHs. The releases of Cs and Ba are similar at pH 1 for the entire leaching time, but are divergent at higher pH, the difference in releases increasing with pH. The Ba leach rate dropped to between 7×10^{-6} g m^{-2} d^{-1} and 2×10^{-5} g m^{-2} d^{-1} for the other pH conditions i.e. pH > 1. The reasoning for the deviation between Cs and Ba releases is provided below in the discussion on static leaching at different SA/V ratios. The Ti concentration for all leachates was below the analytical detection limit (0.02 ppm).

The equivalent alteration thicknesses calculated from the normalized Cs mass loss are plotted against pH in Fig. 3. Except for leaching at pH 1, where the Cs-depleted layer was nearly 300 nm thick, a layer no more than 20 nm thick developed, relatively quickly, and then remained stable over time. It is important to note that these thicknesses were estimated from solution analysis results, consequently rapid dissolution of soluble phases containing Cs could occur without necessarily forming an alteration layer a few tens of nanometers thick. Comparing the normalized Cs and Ba mass losses (Fig. 4) shows increasingly pronounced incongru-

Table 2
TEM/EDS analysis of a pristine hollandite specimen (composition $Ba_1Cs_{0.28}Fe_{0.82}Al_{1.46}Ti_{5.72}O_{16}$)

Pristine hollandite	Cs (at.%)	Ba (at.%)	Al (at.%)	Fe (at.%)	Ti (at.%)	O (at.%)
1	1.04	3.81	5.62	3.50	22.67	63.36
2	0.92	3.67	5.93	3.59	22.49	63.40
3	1.03	4.73	5.28	3.78	22.11	63.06
4	1.04	4.53	5.51	3.96	21.90	63.06
5	0.99	4.47	5.78	3.59	22.05	63.12
6	0.76	3.71	5.79	4.07	22.27	63.41
Average	0.96	4.15	5.65	3.75	22.25	63.24
Standard deviation	0.11	0.47	0.23	0.23	0.29	0.17
Formula units (16 oxygen)	0.24	1.05	1.43	0.95	5.63	16.00
Standard deviation	0.03	0.12	0.06	0.06	0.07	

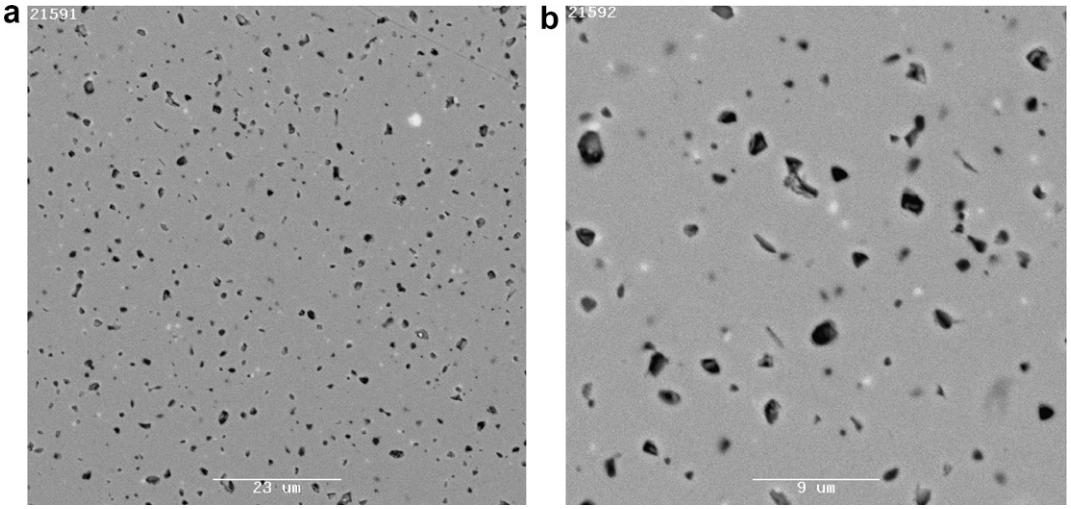

Fig. 1. SEM photomicrographs (in back-scattered electron mode) of un-leached hollandite, showing porosity (as black holes) and the trace Cs–Si-rich phase (light grey, submicron specks).

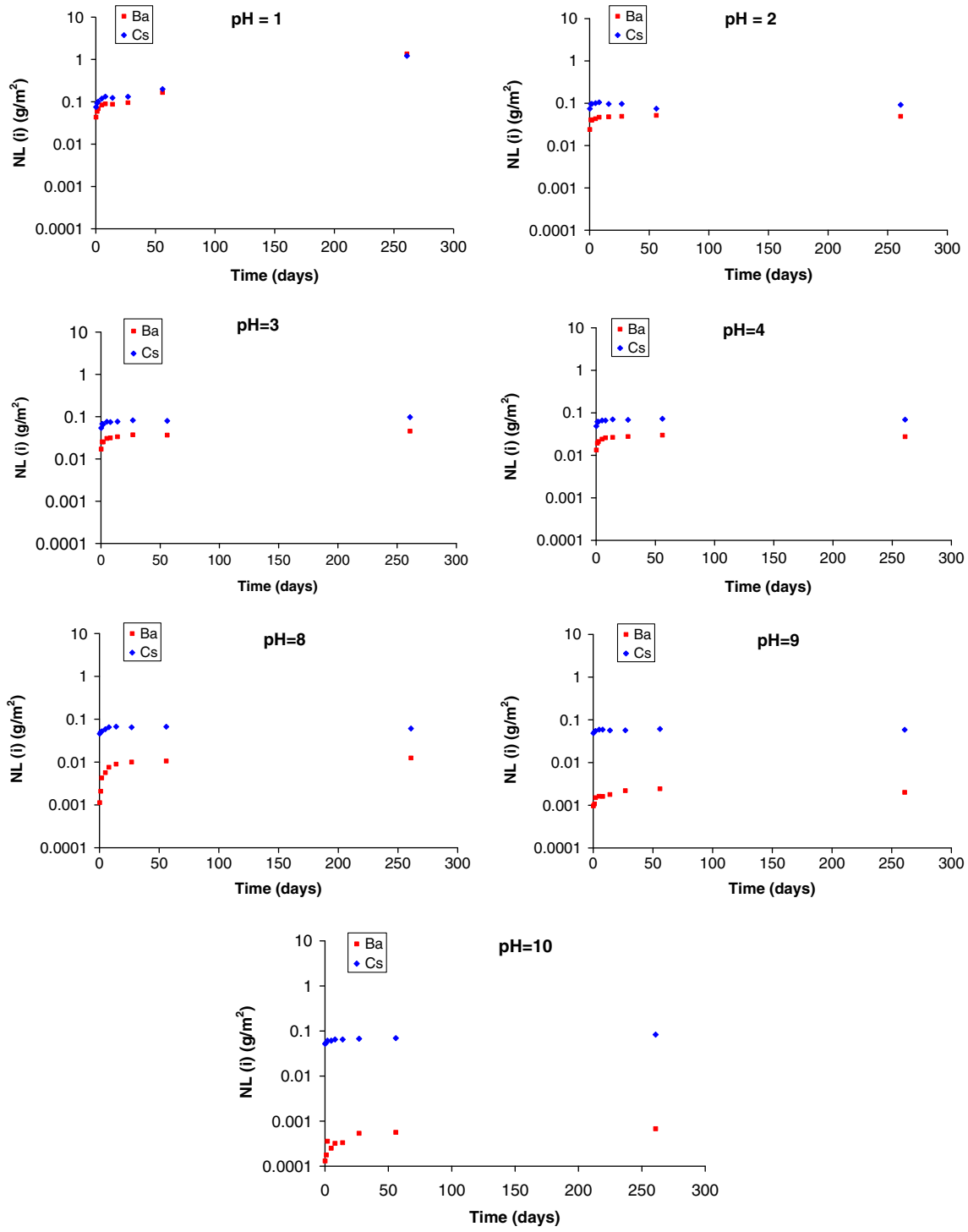

Fig. 2. Normalized Cs and Ba mass loss versus time at different pH values (SA/V = 1 cm^{-1}, 90 °C).

ence as the leaching solution pH increases. As previously described, Cs and Ba were leached congruently at the most acidic pH, whereas at pH 10 the Ba concentration in solution was two orders of magnitude lower than for Cs after 56 days of alteration (similar results were obtained for longer leaching periods).

3.2.2. Static leaching at different SA/V ratios

The normalized Cs and Ba mass losses for SA/V ratios ranging from 0.1 cm^{-1} to 1200 cm^{-1} are shown in Fig. 5. The alteration rates diminished rapidly after the initial release of Cs and Ba. The incongruence between the two elements increased with SA/V ratio, to a maximum of up to three orders of magnitude at 1200 cm^{-1}. Cesium, unlike Ba, was largely unaffected by the SA/V ratio, as demonstrated by the element concentrations in solution that linearly increase with SA/V ratio (see Fig. 6). The relationship between Ba release and SA/V ratio showed a very significant drop in the concentration at 1200 cm^{-1}. Pham et al. [8] found that congruency between Cs and Ba existed for an SA/V ratio range of 2.5–50 cm^{-1}, however, their tests were carried out for just 6 days and at 75 °C.

The release of Cs and Ba during the experiments with variable SA/V ratios could have also been affected by pH. At low SA/V values (up to 1 cm^{-1}), the pH remained near its initial value of 6.5 (see

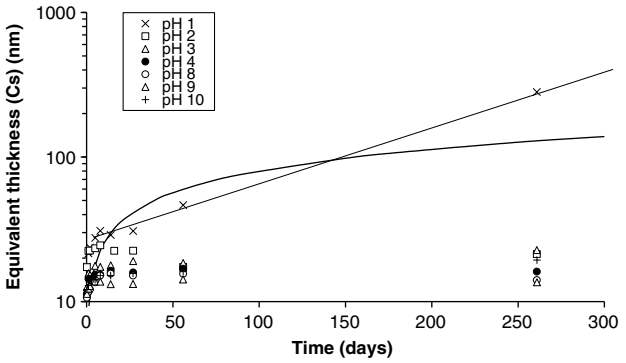

Fig. 3. Equivalent thickness of alteration layer versus time, calculated from normalized Cs mass losses for different pH values (SA/V = 1 cm $^{-1}$, 90 °C). The curve in dotted lines represents a variation with the square root of time, compared with the linear variation (solid line) for the values obtained at pH 1.

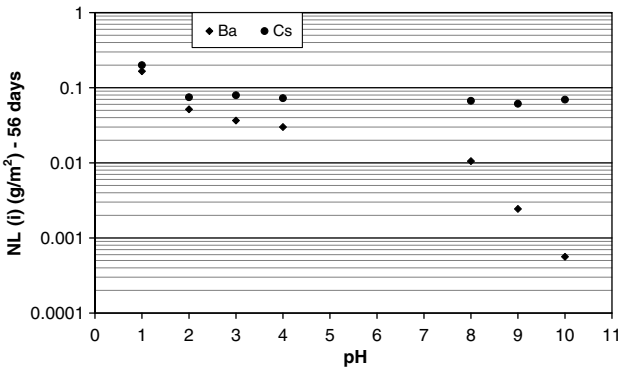

Fig. 4. Normalized Ba and Cs mass losses versus solution pH after 56 days of alteration.

Fig. 7). When the reactive surface area increased, however, leading to higher concentrations in solution, the pH increased, exceeding 8.5 at 1200 cm^{-1}. It is suggested that Ba has precipitated at these higher pH values. This relationship between Cs and Ba releases is similar to that observed in the variable pH experiments in which the incongruence was greater at higher pH values. The higher pH could be related to the solubilization of a large Cs fraction at high SA/V ratios, resulting in a higher exchange with protons in solution. In each experiment, a layer of practically identical thickness (about 20 nm) seems to be depleted in Cs, supporting this hypothesis.

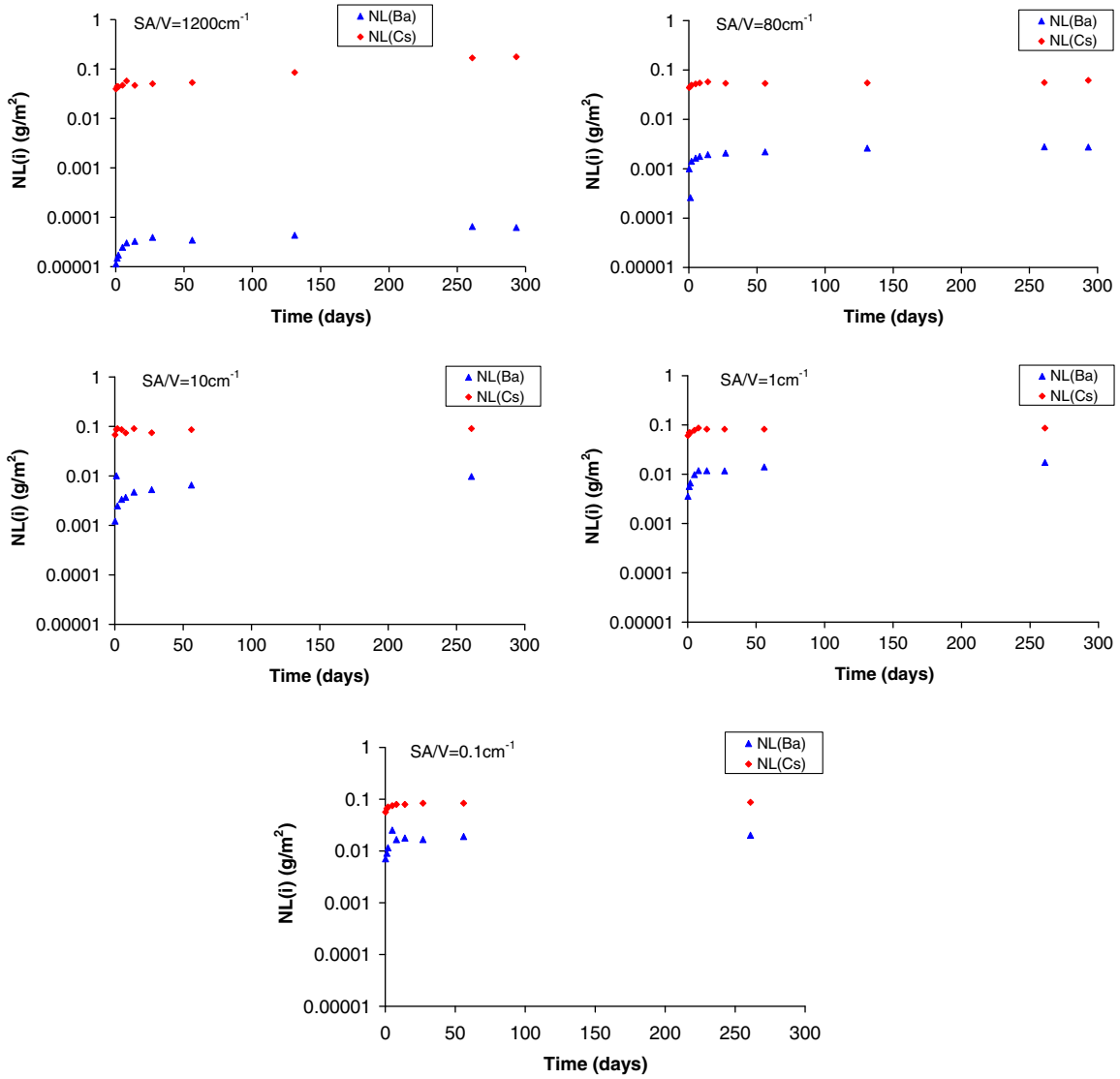

Fig. 5. Normalized Cs and Ba mass losses versus time for different sample-surface-area-to-solution-volume (SA/V) ratios.

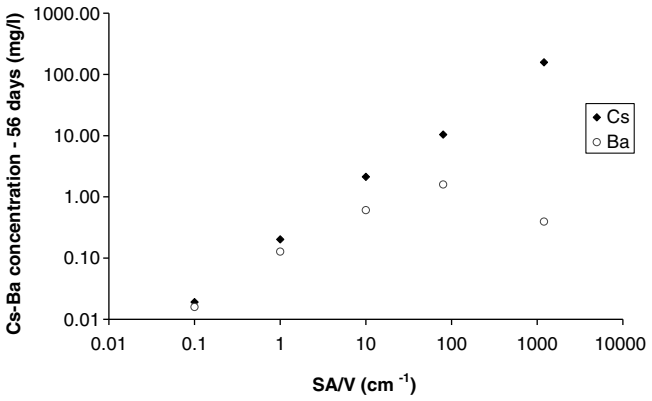

Fig. 6. Concentration Cs and Ba variations in solution versus the SA/*V* ratio after 56 days.

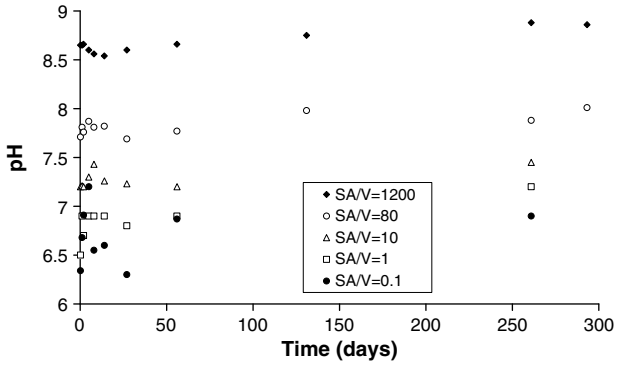

Fig. 7. pH variation at various SA/*V* ratios (cm^{-1}).

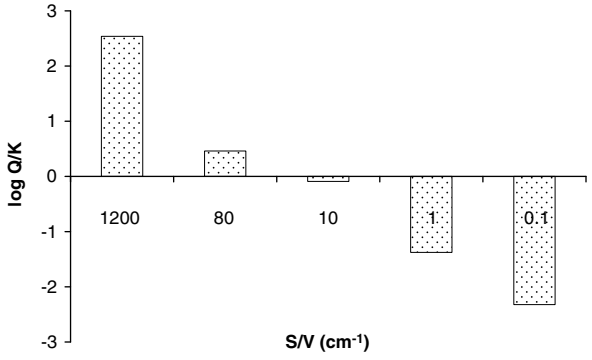

Fig. 8. Saturation index of witherite ($BaCO_3$) calculated with CHESS versus the quantities of elements determined in solution, the pH measured after 56 days, and assuming a CO_2 partial pressure in the atmosphere.

Although the Ba and Cs cations are structurally in a similar configuration within the tunnels of the hollandite and should exhibit comparable behavior during leaching, the stronger apparent retention of Ba compared with Cs at high pH values could be related to the formation of a secondary phase that controls the solubility of Ba. If we consider the simplest phase that could form in the presence of atmospheric CO_2, witherite ($BaCO_3$), Fig. 8 shows the saturation index ($\log Q/K$, ion activity product over solubility constant) for $BaCO_3$ calculated using the geochemical code CHESS[1] from the quantities of elements determined in solution, the pH measured after 56 days, and the CO_2 partial pressure in the atmosphere. The positive values represent oversaturation, hence possible precipitation of the phase.

To verify this hypothesis a leaching experiment was carried out under argon atmosphere in a glove box, to avoid precipitation with atmospheric CO_2, using a pH 10 leachant ($SA/V = 0.1\ cm^{-1}$). Fig. 9 compares the normalized Cs and Ba mass losses in air and in the glovebox – the Cs release was unaffected, whereas Ba was leached at a higher rate without the presence of CO_2. Nevertheless, the Ba mass loss was still more than an order of magnitude lower than that of Cs under argon atmosphere. It is suggested that some of the Ba was consumed in the formation of the $BaCO_3$ phase, and that the remainder was present in a phase incorporating the other spar-

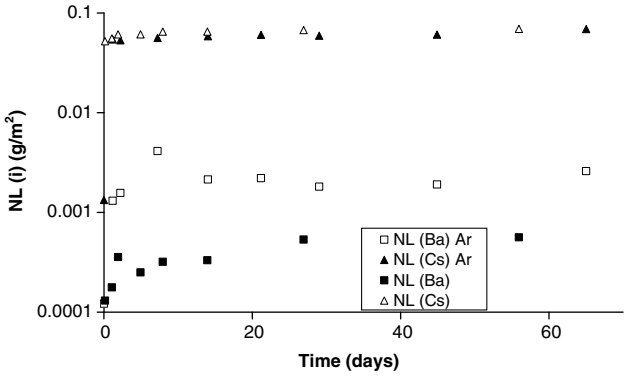

Fig. 9. Normalized Cs and Ba mass losses in air, NL(Ba,Cs), and in argon atmosphere, NL(Ba,Cs)Ar (pH 10, $SA/V = 1\ cm^{-1}$).

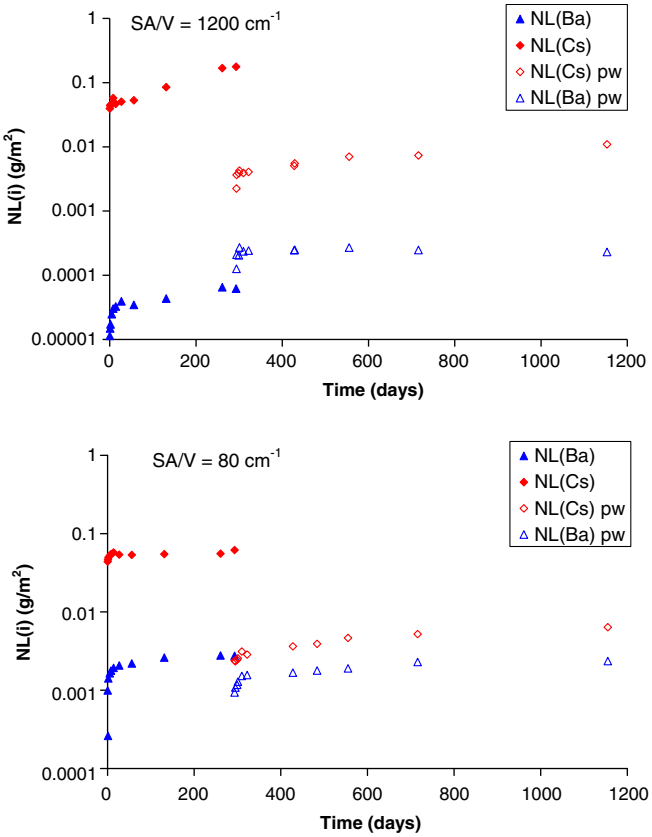

Fig. 10. Normalized Cs and Ba mass losses in pure water for 261 days, then for 894 days after transferring the altered specimen to a fresh pure water solution (pw) (total leaching time exceeding 3 years) at SA/*V* ratios of 1200 cm^{-1} (top) and 80 cm^{-1} (bottom).

[1] http://chess.ensmp.fr/.

ingly soluble elements from the hollandite in which Ba could play a charge-compensating role.

3.2.3. Extended leaching in pure water

To test the response of hollandite leaching behavior to change in leachant conditions (from saturated to unsaturated), a possible scenario in a geological repository context, samples were first leached for 261 days in pure water at SA/*V* ratios of 80 cm^{-1} and 1200 cm^{-1}. They were then removed from the initial solution and leached again (after samples rinsing) in pure water for 894 days (for a total leaching time exceeding 3 years). In replacing the leachates with pure water the instantaneous Cs release dropped sharply and the total quantity in solution was smaller for both SA/*V* ratios (results plotted in Fig. 10). In fact, the release of Cs upon replacing the leachate with fresh water was an order of magnitude lower than the release measured at the beginning of the test, probably due to the Cs-depleted surface layer after leaching for 261 days. The measured concentrations remained very low after leachate replacement, for example, the Cs release corresponds to an altered thickness of less than one nanometer. The Cs leach rates during the last two years were 7.5×10^{-6} g m^{-2} d^{-1} at 1200 cm^{-1} and 3.6×10^{-6} g m^{-2} d^{-1} at 80 cm^{-1}, corresponding roughly to alteration fronts of 0.6 nm/year and 0.3 nm/year, respectively.

After leachate replenishment with pure water, the release of Ba dropped by a factor of 2–3 at the SA/*V* ratio of 80 cm^{-1}, approximately to the same level as at the beginning of the test. To the contrary, at 1200 cm^{-1} the Ba release was slightly greater after leachant replacement. This could be related to the presence of a phase containing Ba that dissolved quickly when the equilibrium in solution was modified by the change to pure water. As mentioned earlier, it is suggested that the $BaCO_3$ phase formed at an SA/*V* ratio of 1200 cm^{-1}. As for Cs, the releases of Ba for both SA/*V* ratios remained fairly constant for the remainder of the leaching time after leachate replacement with the fresh water.

Mass losses became more congruent between Cs and Ba after the leachate replacement.

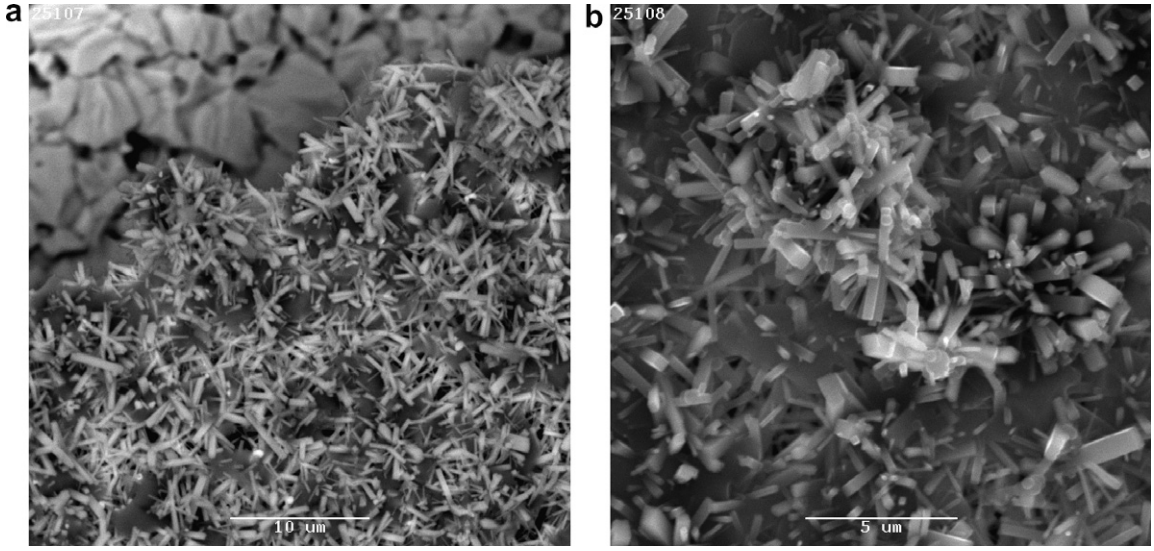

Fig. 11. (a) Secondary acicular titania crystals on primary hollandite substrate in backscattered electron imaging mode (leached at pH 1). (b) More highly magnified photomicrograph of the titania crystals in secondary electron imaging mode.

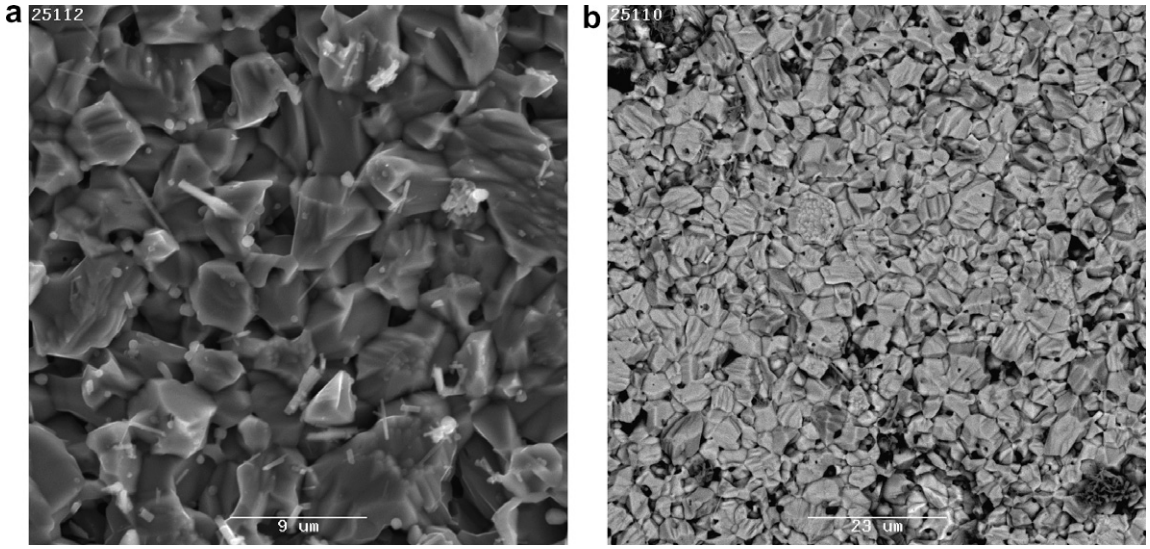

Fig. 12. (a) Photomicrograph of the hollandite substrate in secondary electron imaging mode showing porosity as a result of leaching at pH 1. (b) Primary hollandite substrate in backscattered electron imaging mode showing etching of grain boundaries. Black spots are pores.

3.3. Surface characterization by XRD and SEM/ EDS

SEM analysis showed that for the specimen leached at pH 1, a secondary surface phase, a mixture of acicular TiO_2 crystals and a Na-rich phase, was prevalent (see Fig. 11). The Na-rich phase, later identified as $NaNO_3$, is interstitial to the titania crystals, forming perhaps from leachate droplets entrapped between the crystals upon removal of the specimen from the leachate at the cessation of the experiment. The surface of the specimen is very porous, especially within the titania layer (see Fig. 12(a)). The hollandite substrate beneath the alteration layer generally has distinct grain boundaries (see Fig. 12(b)), probably from the etching effect of the acidic leachant, with a fairly uniform grainsize of 5–10 μm. The hollandite immediately adjacent to the TiO_2 aggregates, as shown in backscattered electron mode, have a slightly different composition (lighter in contrast) to the hollandite elsewhere. The compositional variation could not be detected by EDS. EDS spectra showed Fe associated with the TiO_2.

The hollandite leached at pH 2 exhibits a porous microstructure as a result of leaching, with a Na-rich phase infilling some pores (see Fig. 13(a)). Alteration is evenly distributed over the surface of the specimen. The Na-rich phase is more commonly interstitial to TiO_2 crystals, as for the specimen leached at pH 1. The secondary TiO_2, which also contains Fe, is not as prevalent as for the specimen leached at pH 1 (see Fig. 13(b)). The majority of the specimen surface is covered by Al, Ba-depleted hollandite, with a few areas present of unaltered hollandite (see Fig. 14). The unaltered hollandite is present most commonly in depressed areas of the specimen surface. There are some very fine granules (sub-micron) on the surface of the specimen, most likely very fine particles of hollandite (similar backscattered electron image contrast to the primary hollandite grains).

The hollandite leached at pH 3 also exhibits etched grain boundaries (see Fig. 15). The hollandite was compositionally unaltered. Very fine, in situ particles over the entire surface are almost indistinguishable from the underlying hollandite matrix by back-

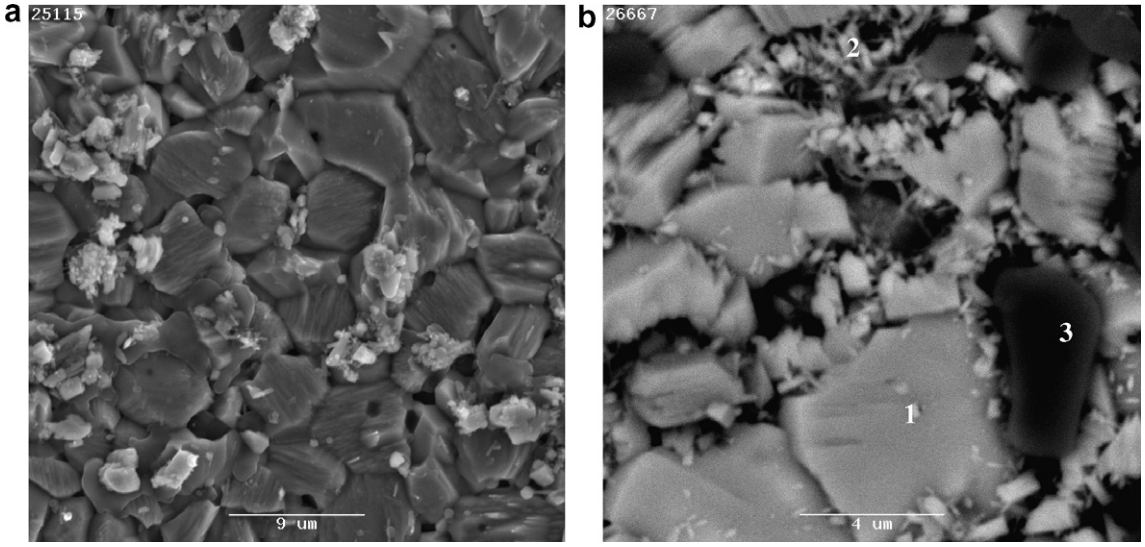

Fig. 13. (a) Secondary electron photomicrograph showing porosity in the hollandite as a result of leaching at pH 2, with some grains of Na-rich phase (light-coloured particles). (b) Backscattered electron image showing primary hollandite (1), acicular titania crystals (2), and the occasional Na-rich phase (3).

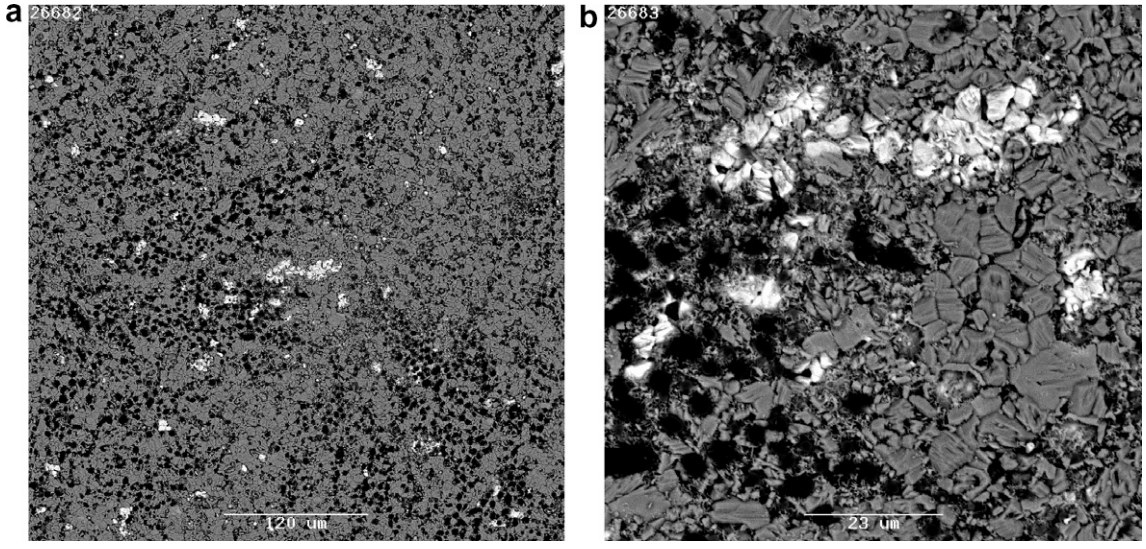

Fig. 14. (a) Low magnification (×200), backscattered electron photomicrograph of the surface of the leached hollandite (at pH 2). The majority of the hollandite is Al- and Ba-depleted (dark grey), with the occasional area of essentially unaltered hollandite (light grey-white). (b) Higher magnification image (×1000) showing the depleted hollandite (dark grey), unaltered hollandite (white), and Na-rich phase (black). Some of the black areas are pores.

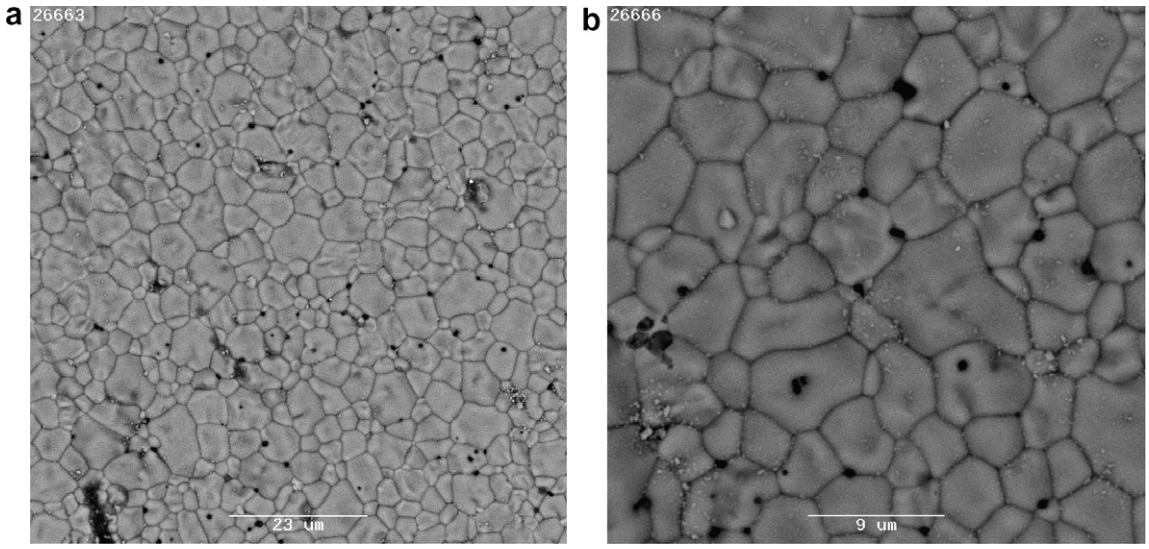

Fig. 15. (a) Lower magnification (×1000), backscattered electron photomicrograph of the surface of the hollandite leached at pH 3 showing well-defined grain boundaries. (b) Higher magnification image (×2500), also in backscattered electron mode. Black areas are pores.

scattered electron imaging, although clearly resolved under secondary electron imaging, so it is most likely to be hollandite (particles are too fine for EDS analysis). The surface of the specimen was analysed by EDS for Na, firstly using a coarse raster scan, then focusing on the large intergranular spaces, however no Na could be detected. There was no evidence of secondary titania as seen under pH 1 and pH 2 leaching conditions.

The specimen leached at pH 4 exhibited similar features to that leached at pH 3 (see Fig. 16). There was no evidence of any compositional alteration of the hollandite, and no secondary products, and finer hollandite particles were distributed over the surface.

The hollandite in the specimen leached at pH 8 shows no sign of compositional alteration, although grain boundary definition is high as for the other leached specimens (Fig. 17(a)). Fines on the surface are assumed to be hollandite due to lack of BEI contrast with the primary hollandite, although difficult to determine if they are in situ or re-deposited. A coarse EDS raster scan of the surface (×2500) shows that Na is present. Closer examination indicates that a Na-rich phase appears to be interstitial to the finer hollandite particles (Fig. 17(b)). This phase is unevenly distributed over the surface of the specimen.

The specimen leached at pH 10 also exhibits fine hollandite particles distributed over the surface (Fig. 18). Several of the grains are sufficiently large for EDS analysis and have the composition of unaltered hollandite.

The testing of the hollandite at the various pHs highlighted the increase in alteration with lower pH. In particular, the hollandite leached at pH 1 and pH 2 was characterised by the alteration of the hollandite with subsequent formation of titania (rutile). This alteration layer was most prominent at the pH 1, with alteration at pH 2 depicted generally as a widespread depletion in Ba and Al of the hollandite, with titania forming interstitially in some areas of the hollandite.

These SEM/EDS observations concur with the leaching results which showed a much greater calculated alteration thickness at pH 1 than for the other pHs.

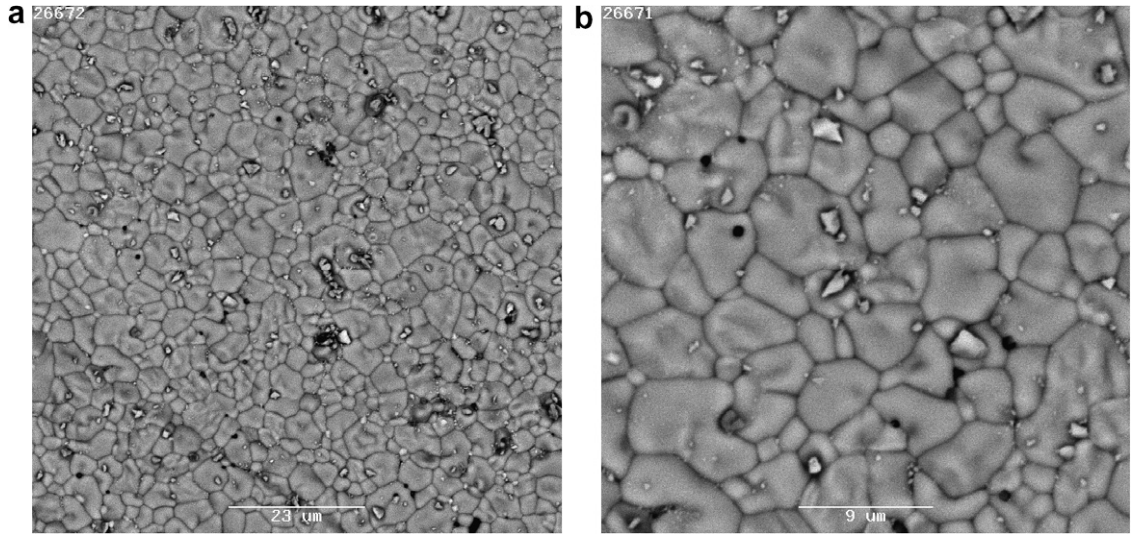

Fig. 16. (a) Lower magnification (×1000), backscattered electron photomicrograph of the surface of the hollandite leached at pH 4 showing well-defined grain boundaries. (b) Higher magnification image (×2500), also in backscattered electron mode. Black areas are pores.

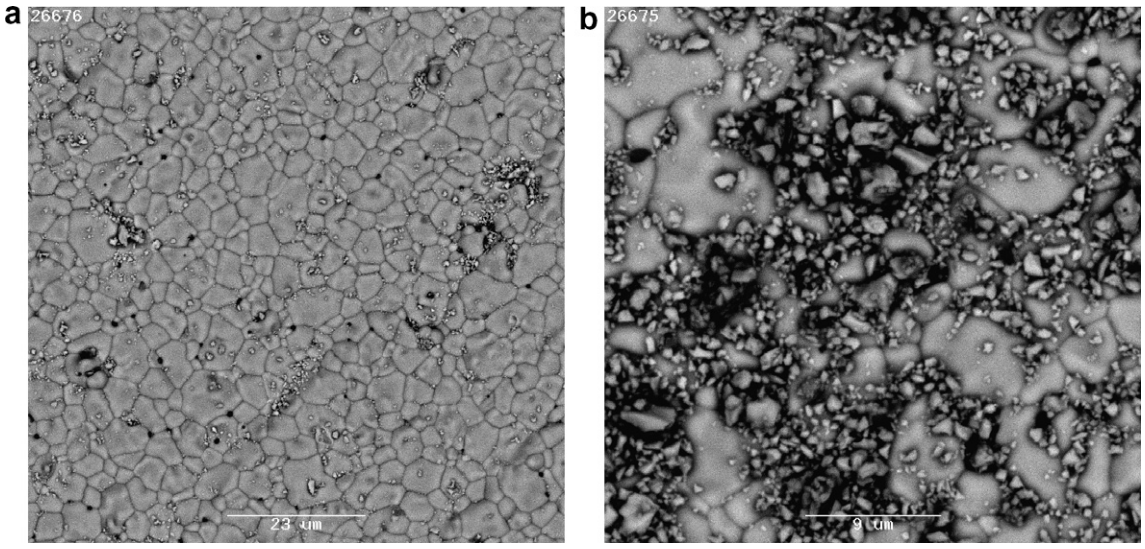

Fig. 17. (a) Backscattered electron photomicrograph of the surface of the hollandite leached at pH 8 showing well-defined grain boundaries. (b) Higher magnification BEI of surface showing hollandite (light grey), primary matrix as well as fines, and interstitial Na-rich phase (black).

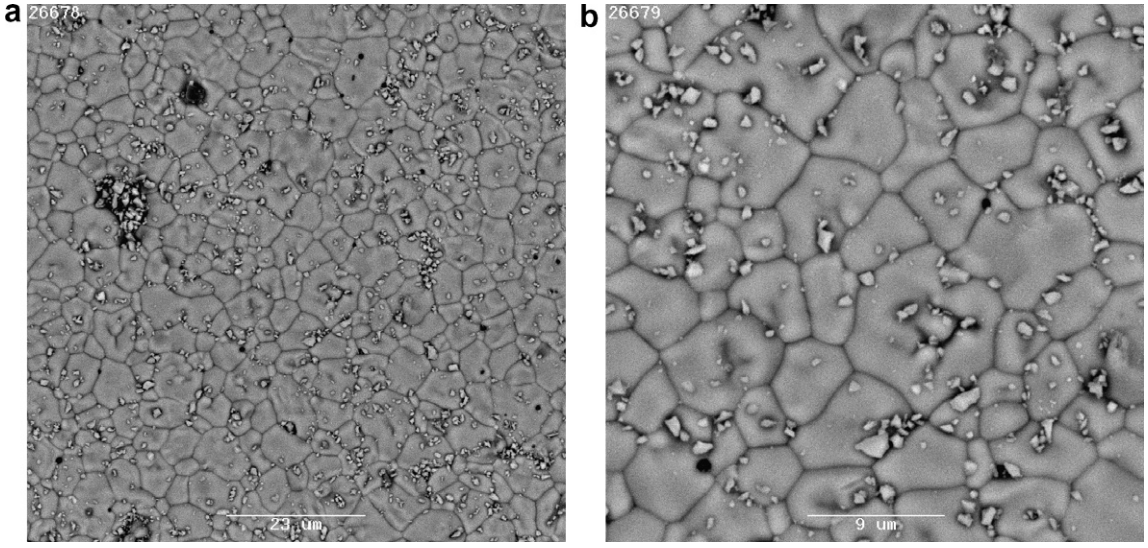

Fig. 18. (a) Backscattered electron photomicrograph of the surface of the hollandite leached at pH 10 showing well-defined grain boundaries. (b) Higher magnification BEI of surface showing hollandite (light grey), as primary matrix as well as fines.

A common feature of most of the hollandite specimens leached at the various pHs, in particular those samples where surface alteration wasn't prominent (pH > 2), was the fairly even distribution of fines. It is likely these fines were a remnant of the sample preparation process, and although would have contributed to the elemental releases during the durability testing, the leach rates calculated would be an overestimation and therefore a conservative representation of chemical durability.

Each of the hollandite specimens leached at the different pH exhibited a yellow colouring, some more intense than others. The colour was most noticeable in the specimens leached at pH 1 and pH 2, and barely discernible at the other pHs. The majority of the yellow alteration layer was scraped from the surface of the specimen leached at pH 2 and analysed by XRD to determine mineralogical composition.

XRD analysis indicated the Na-bearing phase observed in the specimen leached at pH 2 to be a mixture of sodium nitrate ($NaNO_3$) and rutile (TiO_2), although the peaks attributed to rutile were weak. Barium nitrate was also detected in the pH 2 surface alteration layer. As the precipitate on the surface of the specimen leached at pH 1 had a similar appearance (physically and microstructurally) and EDS spectra to that of the specimen leached at pH 2, some of this precipitate was scraped from its surface and placed in boiling deionised water for several hours to dissolve any possible remnant nitrates (highly soluble in water), with the intention of leaving behind the other insoluble phases such as rutile. This residual precipitate was then analysed by XRD for mineralogical composition. Analysis of the precipitate showed it to be rutile with no soluble nitrate phases present. The initial scan showed several very small peaks corresponding to rutile, and the sample was re-analysed to focus on those peaks only (to achieve better resolution). The second scan confirmed the presence of rutile.

The presence of the $NaNO_3$ has formed as a result of using nitric acid, alternating with NaOH, to arrive at the eventual starting pH of the leachant used in the experiments. This has led to the inadver-

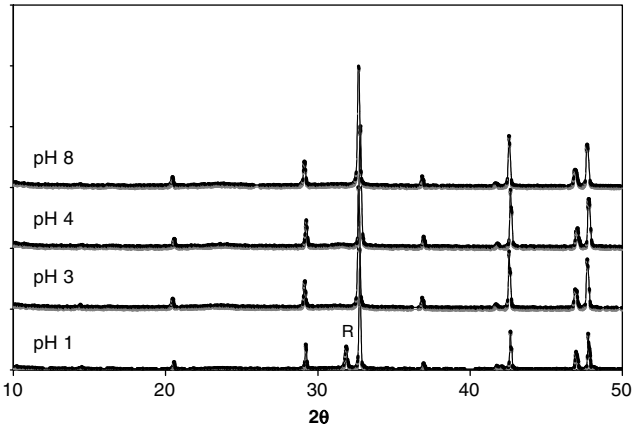

Fig. 19. XRD spectra of the surface of the hollandite specimens leached at the various pHs (primary rutile peak marked as R).

tent formation of $NaNO_3$ on the surface of the specimens, most likely precipitating at the conclusion of the experiments after the specimens were removed from the leachate and air-dried. It is considered that the presence of these ions in the leachates, and the eventual precipitation of $NaNO_3$, has not unduly affected the leaching behavior of the hollandite matrix during the tests. The presence of $Ba(NO_3)_2$ has arisen as a precipitation reaction between Ba released from the hollandite matrix and nitrate from nitric acid addition. It could also impact the noncongruency between the Cs and Ba leaching.

XRD analysis of the surface of the specimens leached at pH 3, 4 and 8 detected no rutile, correlating with SEM findings (see Fig. 19). The specimens leached at pH 9 and 10 were not analysed by XRD, however, it is unlikely, based on other XRD results and SEM findings, that any phase other than hollandite would be present.

The surface characterization studies using XRD and SEM/EDS show that at low pH (<3) secondary rutile forms, most likely via the mechanism proposed by Bursill (outlined earlier). The notion of a continuous reaction front, as proposed by Luca et al. [9], is also supported by the findings presented here.

4. Conclusion

Congruency in Cs and Ba releases from the Fe–hollandite is evident at pH 1 only, with incongruency increasing with pH. The most significant effect on hollandite also occurs at low pH, at least in the longer term. Cs and Ba releases are highest under pH 1 conditions, and for pH > 1 Cs releases appear virtually independent of pH. There is substantial surface alteration of the hollandite at pH 1 with the prevalence of secondary rutile on the leached surface. Alteration of the hollandite is also a feature at pH 2, although the incidence of secondary rutile is less common. At pH 1 the reactive surface of the hollandite is being completely altered to rutile, whereas at pH 2 reactivity of the hollandite is less severe and is more commonly depicted as areas of Al and Ba depletion. The Ba depletion at pH 2 correlates with the higher Ba mass losses measured in the leachates compared with the tests at higher pHs.

In terms of the effect of SA/*V* ratio on hollandite durability, our work has shown that Cs is effectively not affected by SA/*V* ratio i.e. no solubility constraints, whereas it has been pointed out that Ba, in the presence of atmospheric CO_2, could form $BaCO_3$, subsequently precipitating, thereby reducing Ba concentration in the leachates, particularly at higher SA/*V* ratios.

Replenishing leachates generated in the tests at 80 cm^{-1} and 1200 cm^{-1} SA/*V* ratios with fresh deionised water confirmed Cs depletion of the hollandite surface and the likely presence of a secondary soluble, Ba-bearing phase, having formed after leaching in water for 261 days.

Acknowledgements

The authors are grateful to Melody Carter for useful contributions to the XRD analysis and interpretation and Gilles Leturcq for preparing hollandite samples.

References

[1] M. Muthuraman, K.C. Patil, S. Senbagaraman, A.M. Umarji, Mater. Res. Bull. 31 (11) (1996) 1375.
[2] A.E. Ringwood, S.E. Kesson, K.D. Reeve, D.M. Levins, E.J. Ramm, in: W. Lutze, R.C. Ewing (Eds.), Radioactive Waste Forms for the Future, North-Holland, New York, 1988, p. 233.
[3] W.J. Buykx, J. Nucl. Mater. 107 (1) (1982) 78.
[4] V. Aubin-Chevaldonnet, D. Gourier, D. Caurant, S. Esnouf, T. Charpentier, J.M. Costantini, J. Phys. – Condens. Mat. 18 (16) (2006) 4007.
[5] F. Bart, G. Leturcq, H. Rabiller, in: Proceedings of the 105th Annual Meeting and Exposition of the American Ceramic Society, Nashville, USA, 27 April–2 May, 2003.
[6] M.L. Carter, E.R. Vance, D.R.G. Mitchell, J.V. Hanna, Z. Zhang, E. Loi, J. Mater. Res. 17 (10) (2002) 2578.
[7] S. Myhra, D.K. Pham, R.S.C. Smart, P.S. Turnerm, Mat. Res. Soc. Symp. Proc. 176 (1990) 249.
[8] D.K. Pham, S. Myhra, P.S. Turner, J. Mater. Res. 9 (12) (1994) 3174.
[9] V. Luca, D. Cassidy, E. Drabarek, K. Murray, B. Moubaraki, J. Mater. Res. 20 (6) (2005) 1436.
[10] L.A. Bursill, Acta Cryst. B 35 (1979) 30.
[11] S. Brunauer, P.H. Emmett, E. Teller, J. Am. Chem. Soc. 60 (1938) 309.